Raman-active phonons in the quasi-one-dimensional conductor $La_{8-x}Sr_xCu_8O_{20-\delta}$ (x = 1.6, 2.0): polarized Raman spectroscopy and lattice dynamical calculations

1998 J. Phys.: Condens. Matter 10 1643

(http://iopscience.iop.org/0953-8984/10/7/012)

J. Phys.: Condens. Matter **10** (1998) 1643–1654. Printed in the UK PII: S0953-8984(98)86515-6

Raman-active phonons in the quasi-one-dimensional conductor $La_{8-x}Sr_xCu_8O_{20-\delta}$ ($x = 1.6$, 2.0): polarized Raman spectroscopy and lattice dynamical calculations

M V Abrashev†‡, V N Popov‡ and C Thomsen†

† Institut für Festkörperphysik, Technische Universität Berlin, Hardenbergstrasse 36, 10623 Berlin, Germany

‡ Faculty of Physics, Sofia University, BG-1126 Sofia, Bulgaria

Received 31 July 1997, in final form 20 November 1997

Abstract. Ceramic samples of the $La_{8-x}Sr_xCu_8O_{20-\delta}$ perovskite with a chain-like structure were investigated using micro-Raman spectroscopy. The assignment of the lines observed in the spectra to definite atomic vibrations was supported by lattice dynamical calculations based on a shell model. In the spectra with polarizations parallel to the chains a strong background was observed, indicating strongly anisotropic quasi-one-dimensional conductivity of the structure. The effects of the oxygen deficiency on the Raman spectra are also discussed.

1. Introduction

$La_{8-x}Sr_xCu_8O_{20-\delta}$ is an oxygen-deficient perovskite first reported by Er-Rakho *et al* [1]. Its structure is tetragonal, with space group $P4/mbm$ (D^5_{4h}), for $x = 1.6$: $a = 10.840$ Å $\approx 2\sqrt{2}a_p$, $c = 3.861$ Å $\approx a_p$ [1]. The Cu–O framework contains three types of corner-sharing chain along the c-axis which are built up of CuO_6 octahedra, CuO_5 pyramids and CuO_4 squares, respectively, as illustrated in figure 1. La and Sr atoms are distributed statistically on equivalent positions. Most investigations report that the $La_{8-x}Sr_xCu_8O_{20-\delta}$ compounds are single phase for x such that $1.6 < x < 2.0$ [2–4]. These compounds are slightly substoichiometric ($\delta > 0$): the oxygen content decreases as the Sr content increases. The location of the oxygen vacancies in the structure, however, has not been refined even by neutron powder diffraction, but from crystallographic considerations it was suggested that they are probably distributed over the O(1) sites [1].

Transport measurements on ceramics showed that these materials have metallic conductivity (at room temperature it is comparable in magnitude to that of the layered copper superconductors), but they are not superconducting down to 5 K [4–6]. The investigations on [100]-oriented epitaxial thin films [7] and single crystals [8] indicate that the conductivity along the c-axis is in an order of magnitude larger than that in the ab-plane, i.e. the $La_{8-x}Sr_xCu_8O_{20-\delta}$ structure can be considered to be a quasi-one-dimensional conductor.

The substitution of iron for copper (in $La_{8-x}Sr_xCu_{8-y}Fe_yO_{20}$ [9]) or nickel (in $La_{8-x}Ca_xCu_{8-y}Ni_yO_{20}$ [10]) (where $0 \leqslant y \leqslant 2$) in the structure results in the following interesting effects:

(i) Fe and Ni atoms preferentially occupy the Cu3 octahedral positions;

(ii) the oxygen content in substituted samples is stable (a lack of oxygen vacancies);

0953-8984/98/071643+12$19.50

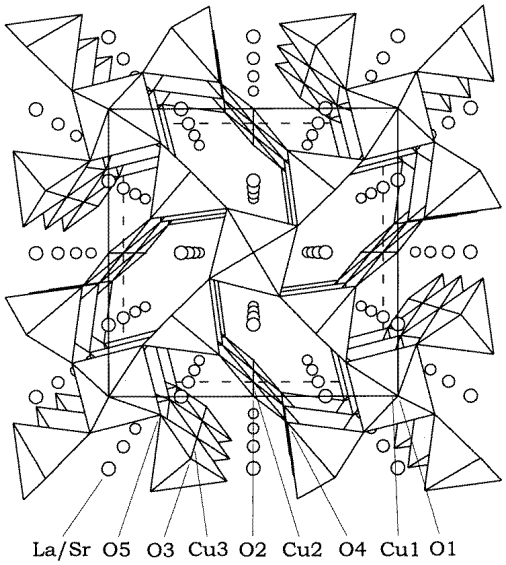

Figure 1. The structure and an elementary cell of $La_{8-x}Sr_xCu_8O_{20}$. The *c*-axis is perpendicular to the sheet. The Cu–O framework is represented symbolically as corner-sharing polyhedra.

(iii) the possibility exists for a wider variation of the hole concentration (a possible larger La/Sr(Ca) ratio), including the observation of a metal–insulator transition.

In this paper we present polarized micro-Raman spectra of $La_{8-x}Sr_xCu_8O_{20-\delta}$ ($x = 1.6, 2.0$). The assignment of the observed lines to definite atomic vibrations is based on lattice dynamical calculations using a shell model. Similarities between some of the modes in the structure and ones in other cuprates are commented on. The effects of the quasi-one-dimensional conductivity and oxygen deficiency on the Raman spectra are discussed.

2. Experimental procedure

The $La_{8-x}Sr_xCu_8O_{20-\delta}$ ($x = 1.6, 2.0$) samples (which will be abbreviated as La6.4 and La6.0, respectively) were prepared using a standard solid-state reaction technique. Appropriate amounts of La_2O_3, $SrCO_3$ and CuO for the nominal compositions were mixed and heated in air for 40 h at 900 °C with one intermediate grinding. The as-obtained materials were ground, pressed into 1 g pellets and sintered at 1000 °C for 24 h. One half of the samples were rapidly quenched from 950 °C to room temperature (La6.4R and La6.0R). The others were slowly cooled for about 12 h (La6.4S and La6.0S).

The lattice parameters determined from x-ray powder diffractograms, obtained with a URD-6 powder diffractometer (Co Kα radiation), are: $a = 10.834$ Å, $c = 3.865$ Å for La6.4S; $a = 10.834$ Å, $c = 3.866$ Å for La6.4R; $a = 10.830$ Å, $c = 3.863$ Å for La6.0S; $a = 10.828$ Å. $c = 3.862$ Å for La6.0R. These values are close to those reported elsewhere (see figure 2). The La6.4R and La6.4S samples are single phase. In the La6.0R and La6.0S samples traces of a secondary phase ($Sr_{14-x}La_xCu_{24}O_{41}$, $x \approx 5$) were identified by x-ray and Raman spectroscopies.

For the microscopic measurements the pellets were polished using 5 μm and 1 μm diamond pastes and then ultrasonically cleaned in an ethanol bath. The Raman spectra were

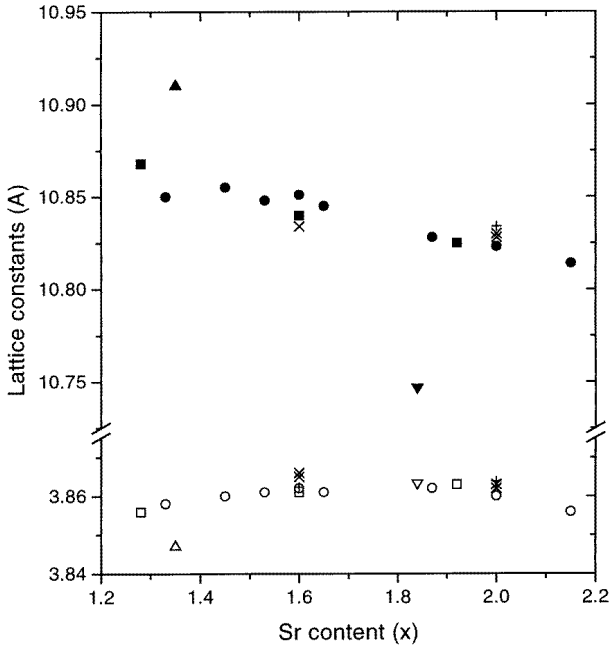

Figure 2. The lattice parameters (a: filled symbols; c: open symbols) of $La_{8-x}Sr_xCu_8O_{20-\delta}$ as a function of Sr content x. □: reference [1]; +: reference [2]; ◯: reference [4]; △: reference [8]; ▽: reference [11]; ×: this paper.

measured using a Labram single-grating spectrometer (DILOR) equipped with an optical microscope, a CCD multichannel detector and appropriate notch filters. A ×100 (×80 for the low-temperature measurements) objective was used to both focus the incident laser beam into a spot of 1–2 μm diameter and collect the scattered light in backscattering geometry. A 632.8 nm He–Ne laser line was used for excitation. To avoid overheating effects the laser power was kept below 1 mW. For the low-temperature measurements the samples were mounted on a cold finger in a He-gas-flow cryostat.

3. Results and discussion

3.1. Classification of the Γ-point modes

The classification of the normal modes at the Γ point of the Brillouin zone is presented in table 1. Four types of Raman-active mode exist in the structure: $7A_{1g} + 7B_{1g} + 7B_{2g} + 7E_g$. The A_{1g}, B_{1g} and B_{2g} modes are vibrations in the ab-plane, whereas the E_g ones are vibrations along the c-axis. Only La/Sr, Cu3, O3, O4 and O5 atoms participate in these modes. The Raman tensors of the four types of Raman-active mode have different nonzero components. In order to identify the Raman line symmetry it is sufficient to obtain polarized Raman spectra from two types of crystal surface: those containing the c-axis and those perpendicular to the c-axis. To separate B_{1g} and B_{2g} modes, additional information about the crystal directions in the surface perpendicular to the c-axis is needed. The notation x, y, z, x' and y' will be used for the [100], [010], [001], [110] and [1$\bar{1}$0] crystallographic directions, respectively. Thus, A_{1g} modes are allowed in zz-, xx- (yy-) and $x'x'$- ($y'y'$-)

Table 1. Normal modes in $La_{8-x}Sr_xCu_8O_{20-\delta}$, $P4/mbm$, $Z = 1$.

Atom	Wyckoff notation	Site symmetry	Normal modes	Remark
La/Sr	8(j)	C_s^h	$2A_{1g} + A_{1u} + 2A_{2g} + A_{2u} + 2B_{1g} + B_{1u} + 2B_{2g} + B_{2u} + 2E_g + 4E_u$	
Cu1	2(a)	C_{4h}	$A_{1u} + A_{2u} + 2E_u$	Octahedral
Cu2	2(d)	D'_{2h}	$A_{2u} + B_{1u} + 2E_u$	Square
Cu3	4(q)	C'_{2v}	$A_{1g} + A_{2g} + A_{2u} + B_{1g} + B_{1u} + B_{2g} + E_g + 2E_u$	Pyramidal
O1	2(b)	C_{4h}	$A_{1u} + A_{2u} + 2E_u$	Octahedral–octahedral
O2	2(c)	D'_{2h}	$A_{2u} + B_{1u} + 2E_u$	Square–square
O3	4(h)	C'_{2v}	$A_{1g} + A_{2g} + A_{2u} + B_{1g} + B_{1u} + B_{2g} + E_g + 2E_u$	Pyramidal–pyramidal
O4	4(g)	C'_{2v}	$A_{1g} + A_{2g} + A_{2u} + B_{1g} + B_{1u} + B_{2g} + E_g + 2E_u$	Pyramidal–square
O5	8(i)	C_s^h	$2A_{1g} + A_{1u} + 2A_{2g} + A_{2u} + 2B_{1g} + B_{1u} + 2B_{2g} + B_{2u} + 2E_g + 4E_u$	Octahedral–pyramidal

Activity		Selection rules for Raman-active modes	Symmetry-allowed directions of vibrations	
			For La/Sr, O5	For Cu3, O3, O4
Raman	$7A_{1g} + 7B_{1g} + 7B_{2g} + 7E_g$	$A_{1g} \rightarrow \alpha_{xx} + \alpha_{yy}, \alpha_{zz}$	In xy-plane	Along $x \pm y$
Infrared	$8A_{2u} + 21E_u$	$B_{1g} \rightarrow \alpha_{xx} - \alpha_{yy}$	In xy-plane	Along $x \mp y$
Acoustic	$A_{2u} + E_u$	$B_{2g} \rightarrow \alpha_{xy}$	In xy-plane	Along $x \pm y$
Silent	$4A_{1u} + 7A_{2g} + 7B_{1u} + 2B_{2u}$	$E_g \rightarrow \alpha_{xz}, \alpha_{yz}$	Along z	Along z

polarizations of the incident and scattered light, B_{1g} modes are allowed in xx- (yy-) and $x'y'$-polarizations, B_{2g} modes are allowed in xy- and $x'x'$- ($y'y'$-) polarizations and E_g modes are allowed in zx- (xz-) and zx'- ($x'z$-) polarizations.

3.2. Identification of the microcrystal orientation

The microcrystals exhibiting the two types of surface necessary for the experiment (namely (001) and ($mn0$) ones) can be easily distinguished on the polished surface of the pellet. The ($mn0$) surfaces are bar shaped with the longer edge along the c-axis; see reference [8]. They also have the strongest optical anisotropy (the greatest change of the colour of the microcrystals during rotation of the pellet when illuminated with linearly polarized white light). Surfaces of the (001) type have square-like shape and they are optically isotropic (due to the tetragonality of the structure). For these surfaces we assume that their edges are parallel to the [110] crystal direction (along the Cu–O bonds in the ab-plane). Some of the microcrystals contain big twins with mutually perpendicular c-axes. At first glance this may appear to mean that at the synthesis temperature the crystals grow as a cubic oxygen-

disordered perovskite and that with decreasing temperature there is a phase transition to a tetragonal oxygen-ordered phase with the formation of twins. However, the elongated rod-like shape of the crystals (some of them with sizes of up to 10 μm $\times$ 50 μm) does not support such a hypothesis. The $La_{8-x}Sr_xCu_8O_{20-\delta}$ crystals probably grow tetragonally, but, due to mechanical stresses during the cooling, oxygen reordering occurs in some crystal regions.

Table 2. Parameters used in the shell model. The O–O short-range potential was taken from reference [13].

Ion	Z ($\|e\|$)	Y ($\|e\|$)	α (Å^3)	Ionic pair	a (eV)	b (Å^{-1})	c (eV Å^6)
La/Sr	2.85	1.70	0.7	La/Sr–O	1500	2.622	0.0
Cu	1.90	3.00	1.3	Cu–O	1500	3.554	0.0
O	−1.90	−3.00	2.0	O–O	22 764	6.711	20.37

3.3. Description of the model used for the lattice dynamics calculations

The model applied is a shell model with the parameters obtained in [12]. In this model the interionic interactions are described by long-range Coulomb potentials and short-range ones, of the Born–Mayer–Buckingham form:

$$V = a\exp(-br) - c/r^6. \tag{1}$$

Here a, b and c are parameters, and r is the interionic separation. The ionic polarizability is also included in the shell model using the simple representation of an ion as a point core with charge Z coupled with a force constant k to a massless shell with charge Y. The values of the model parameters are listed in table 2. As in a previous study of the lattice dynamics of the structurally similar compound $La_4BaCu_5O_{13}$ [14], it was necessary to change the shell charge Y of the O4 and O5 ions from $-3.0|e|$ to $-2.2|e|$, and the free-ionic polarizability α along the z-direction of the same ions from 2.0 Å^3 to 5.0 Å^3, to obtain better correspondence between the calculated and experimental frequencies. The masses and ionic charges of La and Sr ions were substituted for with average values proportional to the (8j) site occupancy.

3.4. Raman-active phonons

The Raman spectra obtained with the sample La6.4S are presented in figure 3. We observed one B_{1g} line (the weak peak at 210 cm^{-1} in the $x'y'$-spectrum) and four B_{2g} lines at 138, 178, 445 and 512 cm^{-1} (see the xy-spectrum). The lines with E_g symmetry have too low an intensity to be detected. We determined the positions of five A_{1g} lines (177, 217, 267, 494 and 535 cm^{-1}) from the xx-spectrum using the fact that additionally allowed B_{1g} lines in that spectrum have negligible intensity compared to the A_{1g} lines. The $x'x'$-spectrum is obviously a superposition of the strong A_{1g} and B_{2g} lines. The lines in the zz-spectrum we will comment on later. A comparison between the experimentally observed and the calculated frequencies of the Raman-active modes is presented in table 3. For the description of the atomic displacements we use the following notation.

(a) The displacements of the atoms belonging to only one pyramid (and the nearest La/Sr atoms to its vertex) are presented. The displacements of the remaining atoms in the unit cell can easily be obtained from the symmetry of the mode.

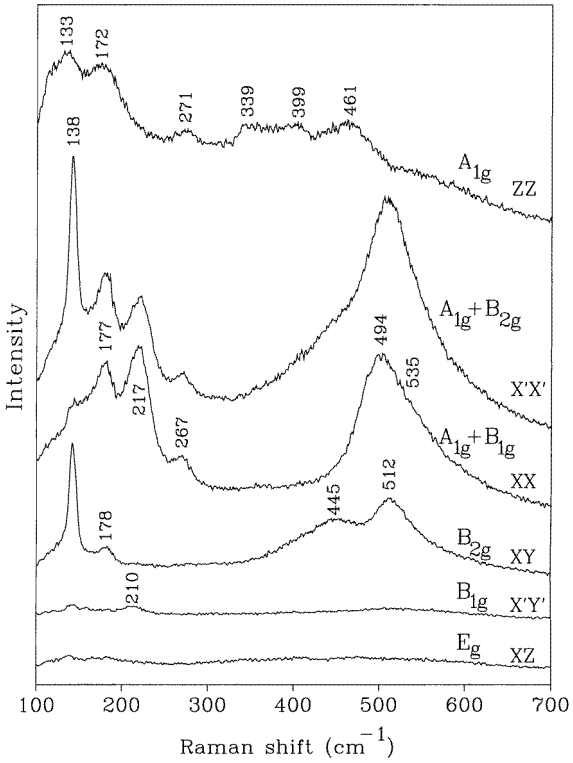

Figure 3. Polarized Raman spectra obtained at room temperature for the sample La6.4S. The scattering configurations and the symmetries of the lines are indicated. $\lambda_L = 632.8$ nm.

(b) For the A_{1g}, B_{1g} and B_{2g} modes (vibrations in the *ab*-plane) the symbols $\parallel$ and $\perp$ indicate the direction of the displacements: parallel and perpendicular to the pyramidal base, respectively.

(c) The signs '+' and '−' indicate their phase (in phase or out of phase).

(d) The atoms are ordered according to their relative amplitudes in the mode.

Before discussing the modes we note several structural similarities with the structures of other cuprates.

(a) The presence of an octahedral chain surrounded by four pyramidal chains is similar to the case for $La_4BaCu_5O_{13}$.

(b) The presence of a square that shares its corners with two pyramids is similar to the structure of $RBa_2Cu_3O_{7-\delta}$ (R: rare earth).

(c) The presence of a square between the bases of two adjacent pyramids along the (110) direction is similar to the structure of $Tl_nBa_2Ca_2Cu_3O_{8+n}$ ($n = 1, 2$).

We will comment in detail only on the modes with relatively simple displacement patterns. The B_{2g} line at 138 cm^{-1} is a pure Cu3 vibration perpendicular to the pyramidal base. This vibration exists in all layered cuprates with two or more Cu–O planes per unit cell (with A_{1g} or A_g symmetry). Its frequency in all cases is close to 140 cm^{-1} and the corresponding line in the Raman spectra is sharp and strong. The line in our spectra has the same features.

Table 3. Experimental (for the sample La6.4S) and calculated frequencies (in cm^{-1}) of the Raman-active modes in $La_{6.4}Sr_{1.6}Cu_8O_{20-\delta}$ ($\delta \approx 0$). For an explanation of the symbols used for the description of the atomic displacements, see the text.

ν_{calc}	ν_{expt}	Assignment	ν_{calc}	ν_{expt}	Assignment
		A_{1g}			B_{2g}
64	—	⊥(+Cu3, +O3), +La/Sr	132	138	⊥(Cu3)
171	177	⊥(+O3, +Cu3), −La/Sr	160	178	⊥(+O3, +Cu3, +O4), +La/Sr
198	217	⊥(−O5, +O3), +La/Sr	219	—	La/Sr
262	267	⊥(+O3, −O5)	301	—	⊥(+O3, −O5)
316	—	⊥(+O3, +O4, +O5)	443	445	⊥(+O4, −O5, −O3)
507	494	⊥(O4)	498	512	⊥(+O3, +O5, +O4)
532	535	∥(O5)	543	—	∥(O5), ⊥(O4)
		B_{1g}			E_g
116	—	∥(+Cu3, +O3, +O5, +O4), +La/Sr	106	—	+La/Sr, +Cu3, +O3, +O5, +O4
120	—	La/Sr	124	—	La/Sr
218	210	∥(+Cu3, +O5, +O3)	192	—	+Cu3, +O3
306	—	∥(O4), ⊥(O5)	322	—	O5
422	—	∥(O3)	329	—	O5
465	—	∥(O4), ⊥(O5)	378	—	O4
504	—	∥(O5)	569	—	O3

The A_{1g} line at 267 cm^{-1} is the out-of-phase vibration of O3 and O5 atoms perpendicular to the pyramidal base. In the layered cuprates with two or more Cu–O planes per unit cell this mode has B_{1g} (or near B_{1g}) symmetry. Its frequency varies over a rather wide range in the different compounds. For the $RBa_2Cu_3O_7$ series, it changes from 347 cm^{-1} to 297 cm^{-1} for R = Lu to La [15]. In $Tl_nBa_2Ca_2Cu_3O_{8+n}$ ($n = 1, 2$) it is near to 240 cm^{-1} [16]. Probably the main factor determining the frequency of this type of vibration is the distance between two adjacent oxygen atoms along the direction of the vibration as well as the phases of their displacements [17]. Here the Cu–O network (the presence of a Cu–O square between the two pyramidal bases) is similar to that in the Tl cuprates and this is a possible explanation for the relatively low frequency for this type of mode.

The A_{1g} line at 494 cm^{-1} is a pure O4 vibration perpendicular to the pyramidal base (i.e. a stretching vibration for the Cu3–O4 and Cu2–O4 bonds). This mode corresponds to the well known A_{1g} (or A_g) 'apex' oxygen mode in the $RBa_2Cu_3O_{7-\delta}$ compounds. The frequency of the latter depends on the type of the rare earth (from 496 cm^{-1} for R = Lu to 525 cm^{-1} for R = La [15]) and the oxygen deficiency (470 cm^{-1} for $\delta = 1$ to 502 cm^{-1} for $\delta = 0$ in $YBa_2Cu_3O_{7-\delta}$ [18]).

The A_{1g} line at 535 cm^{-1}, determined by fitting the region between 400 and 600 cm^{-1} with two Lorentzians, is a pure O5 vibration ('breathing' for the octahedral chains). In the spectrum of $La_4BaCu_5O_{13}$, which contains similar octahedral chains, it was not observed, but its calculated frequency of 531 cm^{-1} [14] is close to the one observed here.

Due to the origin of two of the A_{1g} modes discussed (494 and 535 cm^{-1}) they must be locally sensitive to the change of the number of oxygen vacancies at the O2 and O1 positions, respectively (the nearest oxygen neighbours of O2 are four O4 atoms and the nearest oxygen neighbours of O1 are eight O5 atoms). Surprisingly, the Raman spectra obtained with our four samples (La6.4S, La6.4R, La6.0S and La6.0R) were identical as regards the positions of the lines in accuracy (± 1 cm^{-1}) as well as relative intensity. From this observation we conclude that: (i) the Sr content in $La_{8-x}Sr_xCu_8O_{20-\delta}$ only weakly influences the Raman

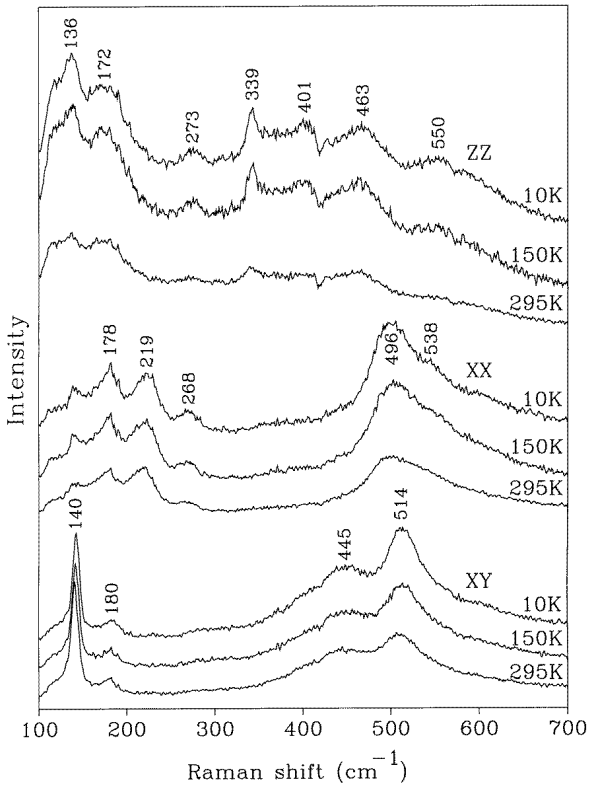

Figure 4. Polarized Raman spectra obtained at different temperatures for the sample La6.4S. The scattering configurations and the symmetries of the lines are indicated. $\lambda_L = 632.8$ nm.

spectra; and (ii) the oxygen contents of the samples are nearly equal and close to 20 (i.e. there is a negligible presence of oxygen vacancies). The small differences between the lattice parameters of the samples support these conclusions.

In some papers, anomalies near 150 K in the temperature dependence of the resistivity [4, 7, 8] and magnetic susceptibility [8] of $La_{8-x}Sr_xCu_8O_{20-\delta}$ were reported. We have not observed, however, any anomaly in the Raman spectra near this temperature (see figure 4). In all of the types of spectra obtained, the lines showed only a slight monotonic shift to higher frequencies on decreasing the temperature.

3.5. Oxygen deficiency and quasi-one-dimensional conductivity effects

As mentioned above, the initial attempts to change the oxygen content of our $La_{8-x}Sr_xCu_8O_{20-\delta}$ samples using different cooling regimes upon their synthesis in air were not successful. The samples obtained had very close lattice parameters and identical Raman spectra. Hauck *et al* [19], on the basis of thermogravimetric measurements, reported a decrease of the oxygen content down to 16.6 in $La_{6.4}Sr_{1.6}Cu_8O_{20-\delta}$ on reaction with hydrogen at temperatures up to 400 °C. However, the reaction of hydrogen with cuprates is a rather complicated chemical process resulting in inhomogeneous metastable samples, rapidly decomposing to secondary products due to water forming in the initial stages of the reaction [21]. For this reason, in order to reduce the oxygen content, we have chosen to

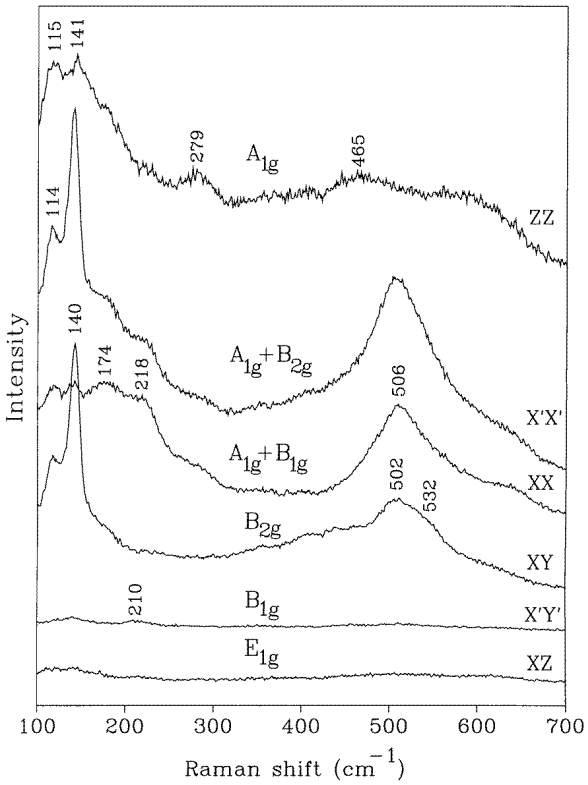

Figure 5. Polarized Raman spectra obtained from large microcrystals (with a size of about 30 μm) for the sample La6.4R after annealing in vacuum at 450 °C for 6 h. The scattering configurations and the symmetries of the lines are indicated. $\lambda_L = 632.8$ nm.

anneal the samples in vacuum. Small pieces of the sample La6.4R containing a part of the polished surface, with the orientation of some microcrystals on it determined in advance, were heated at different temperatures in an evacuated quartz tube for 6 h and then slowly cooled down to room temperature for 12 h. After annealing them at 600 °C we registered the appearance of a secondary phase (CuO) on the surface from the presence of nonpolarized lines at 298, 341 and 632 cm^{-1}, characteristic for this phase in the Raman spectra [20]. After annealing them at 450 °C, however, we did not find any traces of chemical degradation. The modifications of the Raman spectra taken for large crystals (with a size of about 30 μm; see figure 5) are smaller than the ones of the smaller crystals (with a size of about 3–5 μm; see figure 6). The change in colour of the smaller crystals (they became brighter) was larger compared with that for the larger ones. Some of the edges of the large microcrystals as well as the twins in them with the *c*-axis perpendicular to the surface undergo similar changes of colour and the Raman spectra as the small crystals. We interpret these observations in the following manner.

(i) The oxygen deficiency in the microcrystals from the as-treated ceramics is inhomogeneous. It is larger in the small microcrystals and near to the boundaries of the large microcrystals and smaller near their middle due to the finite diffusion rate of oxygen from their core to the surface partly compensating the oxygen reduction.

(ii) The presence of twins with different oxygen contents in one and the same

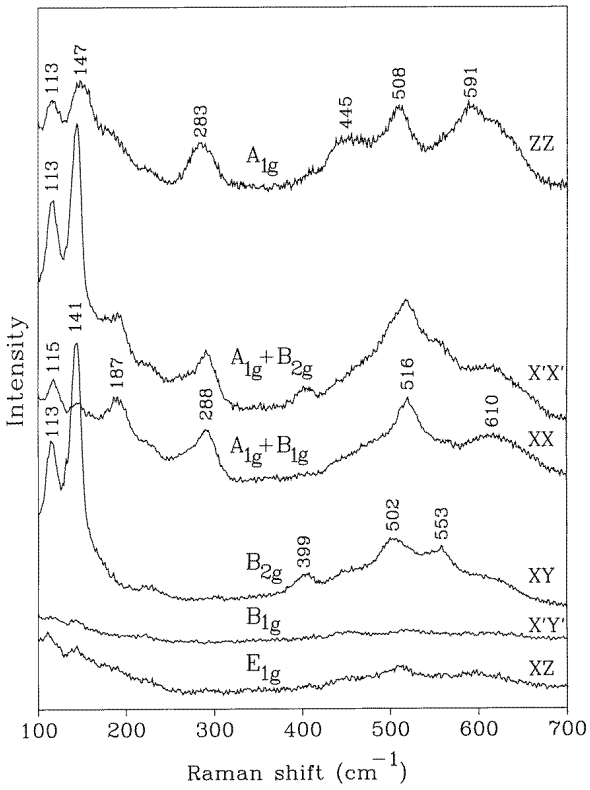

Figure 6. Polarized Raman spectra obtained for small microcrystals (with a size of about 3–5 μm) of the sample La6.4R after annealing in vacuum at 450 °C for 6 h. The scattering configurations and the symmetries of the lines are indicated. $\lambda_L = 632.8$ nm.

microcrystal is clear evidence for the strong anisotropy of the oxygen diffusion in the structure—it is easier along the *c*-axis due to the existence of channels of unoccupied crystal positions in this direction.

Thus, figures 3, 5 and 6 show qualitatively the changes in the Raman spectra with increasing oxygen deficiency. Most of the lines shift their position to higher frequencies: B_{2g}—from 138 to 141 cm^{-1}; A_{1g}—from 177 to 187 cm^{-1}; A_{1g}—from 267 to 288 cm^{-1}; A_{1g}—from 494 to 516 cm^{-1}. These shifts are probably connected with the shortening of the interatomic distances in the *ab*-plane. The large positive shift of the latter line (the O4 vibration perpendicular to the pyramidal base) indirectly supports the hypothesis that the oxygen vacancies occupy the O1 than O2 positions [1]. One of the lines, B_{2g} at 512 cm^{-1}, however, has a negative shift to 502 cm^{-1}. Some of the lines practically disappear: the A_{1g} line at 217 cm^{-1}; the B_{2g} one at 445 cm^{-1}; and the A_{1g} one at 535 cm^{-1}. Three new lines appear with B_{2g} symmetry: at 553, 399 and 113 cm^{-1} (the latter is seen in the xx-spectrum, too) and one with A_{1g} symmetry at 610 cm^{-1} in the spectra of the oxygen-deficient sample. The B_{2g} line at 553 cm^{-1} should be assigned to the calculated mode at 543 cm^{-1}, not observed in the untreated samples. The A_{1g} line at 610 cm^{-1} is probably the forbidden oxygen stretching vibration of O1 (or O2) atoms along the *c*-axis, observed also in oxygen-deficient $YBa_2Cu_3O_{7-\delta}$, containing vacancies in the chains [22, 23]. The other

two lines are incompatible with the modes for the parent $P4/mbm$ structure.

Finally, we comment on the spectra obtained for polarization parallel to the chains (zz). A large background (higher in intensity than the strongest lines observed in the spectra with other types of polarization) superimposed with relatively weak lines was observed in the zz-spectra. The background is equally intense in the spectra of all of the samples, even those that were annealed in vacuum. A similar background was also observed in the spectra of the layered cuprates with polarizations parallel to the Cu–O planes. Although the origin of this scattering continuum was not clarified in detail, it is indisputable that its appearance is connected with their low-dimensional conductivity. Slakey *et al* [24] showed that in the Raman spectra of untwinned $YBa_2Cu_3O_7$ single crystal, this background is more intense in the yy-spectrum (with polarization parallel to the chains and plains) than in the xx-spectrum (perpendicular to the chains and parallel to the planes) and interpreted this as an additional impact of the conducting chains on this scattering. The appearance of this background only in the zz-spectra of $La_{8-x}Sr_xCu_8O_{20-\delta}$ is Raman scattering evidence for the strongly anisotropic quasi-one-dimensional conductivity of this compound. The existence of this background in the spectra of vacuum-annealed samples suggests that they are metallic as well.

It is rather difficult to analyse the origin of the weak lines superimposed with the strong background in the zz-spectra of the samples. All of the lines appear at frequencies different from the ones observed for the other types of spectrum. On the basis of the lattice dynamical calculations, however, we cannot assign any of them to the two unobserved A_{1g} modes. Three of these lines (namely those at 133, 172 and 271 cm^{-1}; see figure 3) have frequencies that are close to but slightly shifted from the lines observed in the other types of spectrum (138, 177 and 267 cm^{-1}). Such a shift in the spectra with a background (usually accompanied with an asymmetric Fano shape of the line) was observed for layered cuprates, and it was explained as indicating an interaction of the corresponding phonons with the scattered electronic continuum [25]. Taking into consideration the fact that these three modes are mainly vibrations of Cu3 and/or O3 atoms, this supports the hypothesis that the carriers exist in the Cu3–O3 pyramidal chains [7].

Acknowledgments

We thank L N Bozukov and M Surtchev for making the x-ray diffraction measurements. MVA acknowledges financial support from the Alexander von Humboldt Foundation (Bonn, Germany). He thanks the Institut für Festkörperphysik (TU-Berlin) for hospitality. This work was supported in part by Grant F530 (NIS 2241) from the Bulgarian National Science Fund.

References

[1] Er-Rakho L, Michel C and Raveau B 1988 *J. Solid State Chem.* **73** 514
[2] Murayama N, Sakaguchi S, Wakai F, Sudo E, Tsuzuki A and Torii Y 1988 *Japan. J. Appl. Phys.* **27** L55
[3] De Leeuw D M, Mutsaers C A H A, Geelen G P J and Langereis C 1989 *J. Solid State Chem.* **80** 276
[4] Tamegai T and Iye Y 1989 *Physica* C **159** 181
[5] Michel C, Er-Rakho L and Raveau B 1988 *J. Phys. Chem. Solids* **49** 451
[6] Torrance J B, Tokura Y, Nazzal A and Parkin S S P 1988 *Phys. Rev. Lett.* **60** 542
Tokura Y, Torrance J B, Nazzal A I, Huang T C and Ortiz C 1987 *J. Am. Chem. Soc.* **109** 7555
[7] Enomoto Y, Murakami T, Iwata T and Moriwaki K 1990 *Phys. Rev.* B **42** 6773
[8] Watanabe T and Matsuda A 1991 *Japan. J. Appl. Phys.* **30** L985
[9] Genouel R, Michel C, Nguyen N, Hervieu M and Raveau B 1995 *J. Solid State Chem.* **115** 469

[10] Roberts G L, Cava R J, Carter S A, Krajewski J J and Peck W F Jr 1996 *J. Solid State Chem.* **121** 319
[11] Lee J Y, Kim J S, Swinnea J S and Steinfink H 1990 *J. Solid State Chem.* **84** 335
[12] Popov V N 1995 *J. Phys.: Condens. Matter* **7** 1625
[13] Catlow C R A, Mackrodt W C, Norgett M J and Stoneham A M 1977 *Phil. Mag.* **35** 177
[14] Abrashev M V and Popov V N 1995 *J. Phys.: Condens. Matter* **7** 4967
[15] Rosen H J, Macfarlane R M, Engler E M, Lee V Y and Jacowitz R D 1988 *Phys. Rev.* B **38** 2460
[16] Burns G, Crawford M K, Dacol F H and Herron N 1990 *Physica* C **170** 80
[17] Abrashev M V, Hadjimitov V N, Bozukov L N and Iliev M N 1995 *Solid State Commun.* **93** 563
Abrashev M V, Thomsen C, Popov V N and Bozukov L N 1997 *Physica* C **274** 141
[18] Feile R 1989 *Physica* C **159** 1
[19] Hauck J, Bischof B, Mika K, Janning E, Libutzki H and Plewa J 1993 *Physica* C **212** 435
[20] Chrzanowski J and Irwin J C 1989 *Solid State Commun.* **70** 11
Hagemann H, Bill H, Sadowski W, Walker E and Francois M 1990 *Solid State Commun.* **73** 447
[21] Hirata T 1996 *Phys. Status Solidi* a **156** 227 and references therein
[22] Thomsen C, Cardona M, Gegenheimer B, Liu R and Simon A 1988 *Phys. Rev.* B **37** 9860
[23] Ivanov V G, Iliev M N and Thomsen C 1995 *Phys. Rev.* B **52** 13 652
[24] Slakey F, Cooper S L, Klein M V, Rice J P and Ginsberg D M 1989 *Phys. Rev.* B **39** 2781
[25] Thomsen C 1991 *Light Scattering in Solids VI* ed M Cardona and G Güntherodt (Heidelberg: Springer) p 285